# Effect of Bi additive on the physical properties of Ge<sub>2</sub>Se<sub>3</sub>-based equichalcogenide glasses and thin films

Roman Golovchak<sup>a\*</sup>, Jarres Plummer<sup>a</sup>, Andriy Kovalskiy<sup>a</sup>, Adam Ingram<sup>b</sup>, Andrzej Kozdras<sup>b</sup>, Tetyana Ignatova<sup>c</sup>, Anthony Trofe<sup>c</sup>, Catherine Boussard-Pledel<sup>d</sup>, Bruno Bureau<sup>d</sup>

<sup>a</sup>Department of Physics, Engineering and Astronomy, Austin Peay State University, Clarksville, TN 37044, USA

<sup>b</sup> Faculty of Physics, Opole University of Technology, Opole, 45-370, POLAND

<sup>c</sup>Department of Nanoscience, Joint School of Nanoscience and Nanoengineering, University of North Carolina at Greensboro, Greensboro, NC 27401, USA

<sup>d</sup>Équipe Verres et Céramiques (V&C), ISCR CNRS UMR 6226, Université de Rennes 1, Rennes, 35042, FRANCE

\*E-mail: holovchakr@apsu.edu

ABSTRACT: The influence of Bi on a structure and physical properties of Ge<sub>2</sub>Se<sub>3</sub>-based equichalcogenide glasses and thin films is studied. Thermal analysis shows increased crystallization ability for Bi-modified glasses. Direct Current (DC) and Alternating Current (AC) electrical conductivity for bulk glasses and thin films is investigated in a broad range of temperatures and frequencies, showing strong dependence on the presence of Bi modifiers. Exposure wavelength dependence of photocurrent is studied at different temperatures for the visible range of spectrum, and correlated with the existence of localized states in the mobility gap of these amorphous semiconductors. Structural peculiarities of the obtained thin films and bulk samples are assessed from X-ray Diffraction (XRD) and high-resolution X-ray Photoelectron Spectroscopy (XPS) measurements. Optical, electrical and thermal properties are shown to be suitable for various applications in photonics, electronics and sensor systems.

**KEYWORDS:** Chalcogenide glass, AC/DC conductivity, photosensitivity, wavelength dependence, temperature dependence.

## INTRODUCTION

Chalcogenide glasses (ChG) are considered as convenient and cost-effective media for various applications in modern photonics and electronics, mostly because of their high IR transparency, excellent fiber drawing and molding capabilities, large optical nonlinearities, semiconductor properties and Ovonic effect. A number of bulk glasses and thin films have been proposed recently for applications in far-IR optics, optical waveguides for space telecommunication, sensor technologies, phase-change memory devices, rechargeable batteries and Ovonic switches. The ChG compositions are being continuously improved in order to optimize the efficiency and functionality of the devices. As a rule, the refinement is achieved by changing the ratio between constituent chemicals or by mixing with new chemical elements. Using this approach, most of the binary and ternary ChG systems have been studied, and

compositional dependences of major physical/chemical properties have been documented throughout their entire glass-forming regions. 9-11 Mixing more than three constituents in multicomponent ChG composition opens a wider range of possibilities for the improvements and tailoring the medium properties, but simultaneously complicates the understanding of ChG structure. Recent advances in the multicomponent ChG have led to the discovery of so-called "equichalcogenide" family (ChG containing three chalcogens S, Se and Te simultaneously) with unique properties that can be explored in the all-chalcogenide photonic/electronic integrated platforms. 12,13 The multifunctional platforms that are based on a single-family material are very appealing, because they can combine various effects in one medium using same technological process. In particular, it is shown that amorphous materials of Ge-Sb-S-Se-Te equichalcogenide family can combine a high thermal stability, IR transparency, high sensitivity to the external influences (radiation, light, temperature)<sup>13</sup> and phase-change memory effect.<sup>12</sup> Their physical and chemical properties can be further improved using nanoscale design, which opens an entirely new range of functionalities. In this regard, addition of Bi can lead to useful nanoscale modifications by changing type of conductivity, trigger local crystallization of amorphous matrix or create partially ordered nanoscale inclusions like the formation of  $Bi_2Se_nTe_{3-n}$  (n = 0, 0.5, 0.6, 1, 2) mixed crystallites in Bi-modified Ga-containing GeSe<sub>4</sub>-GeTe<sub>4</sub> glasses, which led to a giant infrared and visible light attenuation effect. <sup>14</sup> Thus, it was shown previously that Bi in low concentrations (less than ~1 at.%) can form topological coordination defect pairs Bi<sub>4</sub><sup>+</sup> - Se<sub>1</sub><sup>-</sup> in Se-rich networks, <sup>15</sup> while at higher concentrations it enters glass networks of Ge-Se and As-Se glasses in the form of BiSe<sub>3/2</sub> pyramids. <sup>16</sup> These pyramids can form dispersed partially ordered nanophases, which interpenetrating network may be a reason for the percolative conductivity behavior and the conductivity type reversal in ChG, as well as thermoelectric behavior. 16 However, the influence of Bi additives on the properties of complex chalcogenides, like those containing all three chalcogens (S, Se and Te)

simultaneously in their structure, has not been investigated. Even the basic physical properties (mechanical, thermal, electrical, optical) are not studied in these semiconducting materials yet.

In this work, the influence of Bi additives on the optical, thermal and electrical properties of Ge<sub>2</sub>Se<sub>3</sub>-based equichalcogenide glass matrix is studied. Ge<sub>2</sub>Se<sub>3</sub> composition is chosen as it belongs to the second Ge-rich glass-forming region of Ge-Se system.<sup>9,10</sup> While the glass-forming region for Ge-Se-Te-S quaternary system is not established yet, the ones for ternary Ge-Se-S, Ge-Se-Te and Te-Se-S systems are tight to the Se-rich domains.<sup>10</sup> So, we kept the total Se content in our compositions at the level of 46-48 at.%.

#### **EXPERIMENTAL SECTION**

The (Ge<sub>2</sub>Se<sub>3</sub>)<sub>10</sub>Se<sub>18</sub>Te<sub>16</sub>S<sub>16</sub> (HC0) and Bi<sub>5</sub>(Ge<sub>2</sub>Se<sub>3</sub>)<sub>10</sub>Se<sub>15</sub>Te<sub>15</sub>S<sub>15</sub> (HC5) glasses were prepared by conventional melt quenching method using high-purity elements (5N or better). The appropriate amounts of precursors with total mass ~25 g were vacuum-sealed in silica ampoules of 10 mm in diameter. They were heated up to 900°C with 2°C/min heating rate, homogenized at this temperature for 12 hours in rocking furnace and then quenched from 700°C into room temperature water. To relieve the mechanical strains appeared as a result of rapid quenching, the specimens were additionally annealed at 100 °C for 3h.

Thin films were prepared in high vacuum using MBRAUN thermal evaporator and small chunks of bulk HC0 or HC5 materials loaded into tungsten boat as evaporation source. Thickness (~1 µm) of the films was monitored using quartz crystal microbalance method implemented into MBRAUN evaporator system. Microscopy glass slides were used as substrates that were mounted on the rotating holder of the evaporator.

XRD patterns were measured with Rigaku Miniflex 6G system (Cu  $K_{\alpha}$  X-ray source ran at 40 kV and 15 mA, patterns collected with 0.01 degree step), equipped with an accessory for thin film XRD measurements at different temperatures. The high-energy XRD experiment was performed at the beamline 11-ID-B, Advanced Photon Source, Argonne National Laboratory,

using X-rays with wavelength 0.2127 Å and position sensitive Perkin Elmer amorphous silicon detector. These measurements were carried out at room temperature using coarse powdered (with mortar and pestle) sample sealed in Polyimide capillaries.

Mettler Toledo DSC1 equipped with FRS5+ sensor and TC100 intercooler was used for conventional differential scanning calorimetry (DSC) and TOPEM® measurements. The DSC data were recorded in heating mode (2,5,10,20,30 K/min heating rates), using inert atmosphere and ~10 mg samples sealed in standard aluminum crucibles. TOPEM® data were obtained using an average heating rate of 1 K/min, a temperature modulation pulse height of 1 K, and a window width of 15 to 40 seconds.

X-ray photoelectron spectroscopy (XPS) data were obtained using a high-resolution ESCALAB Xi+ spectrometer (Thermo Electron North America LLC) equipped with a monochromatic Al  $K_a$  (1486.6 eV) X-ray source under a vacuum of  $10^{-8}$  Torr (or better). The surface of the samples was cleaned with a quick Ar-ion sputtering to remove surface contaminations directly before the measurements. The surface charging from photoelectron emission was neutralized using a low energy (<10 eV) electron flood gun. The experimental positions of the valence band and core level spectra were adjusted by referencing to the position of 1s core level peak (284.6 eV) of adventitious carbon. YPS data were analyzed with standard CASA-XPS software package, using Shirley background and a pseudo-Voigt line shape (mix in the Gaussian/Lorentzian product form was fixed to 0.3) for the core level peaks.

DC photoconductivity measurements were performed using the investigated film in series with Keithley 485 pico-ammeter and Agilent E3631A power supply. A correction on the dark photocurrent was applied before each measurement. The relative change in current (*RCC*) was calculated as  $RCC = \frac{I_{photo} - I_{dark}}{I_{dark}} * 100\%$ , where  $I_{photo}$  and  $I_{dark}$  are photocurrent and dark current values, respectively. Parallel carbon paste electrodes (1 cm long with a gap of 1 mm) were used to create an electrical contact with the film. A temperature-controlled vacuum

chamber, Linkam (L-THMS350/EV-4), was used to mount the films during light exposure. The chamber was purged with pure nitrogen gas to reduce oxidation processes at the elevated temperatures. The samples were exposed through the chamber's quartz window to various wavelengths of light ranging from 400 to 1000 nm and at various temperatures ranging from 223 to 398 K. Light for the exposure was obtained using a xenon short arc lamp of Horiba Fluorolog-3 spectrofluorimeter equipped with a grating monochromator. An appropriate set of filters has been used to cut higher orders diffraction maxima from the exposure spectrum, verified using the VIS spectrometer (Ocean Optics). The power of the incident light was controlled by a slit width of the spectrofluorimeter and measured with a power meter (Thorlabs PM100 with S130A sensor) placed directly at the location of the sample. It was chosen to keep a constant number of photons per second (flux) for each wavelength of the incident light. Temperature dependences of AC (4Hz to 8 MHz frequency range) and DC conductivity were obtained using HIOKI LCR meter with a bias voltage of 1 V. Real (Z') and imaginary (Z'') parts of measured complex impedance (Z) were used to calculate complex dielectric constant (E' and E'') and electric modulus (E' and E'') and electric modulus (E' and E'') and different frequencies E'

$$\varepsilon' = \frac{Z''}{|Z|^2 \omega \varepsilon_0} \frac{d}{S} , \quad \varepsilon'' = \frac{Z'}{|Z|^2 \omega \varepsilon_0} \frac{d}{S}$$
 (1)

$$M' = \frac{\varepsilon'}{\varepsilon'^2 + \varepsilon''^2}, \quad M'' = \frac{\varepsilon''}{\varepsilon'^2 + \varepsilon''^2}$$
 (2)

where d is the distance between electrodes, S is an area of the contact,  $\varepsilon_0$  is the electric permittivity of free space.

Optical transmission spectra were measured at room temperature by Avantes (AvaSpec-ULS2048XL-2) UV/VIS fiber optic spectrometer, and used for absorption coefficient and optical bandgap calculations.

#### RESULTS AND DISCUSSION

Bulk samples of HC0 and HC5 glasses showed no evident crystalline reflexes in the conventional XRD patterns at room temperature, testifying on an overall good vitreous nature of the prepared bulk materials. In the case of Bi-modified composition HC5, the high-energy synchrotron XRD patterns were additionally collected on bulk samples (Fig. 1) to obtain more precise information on the possible crystallites (or ordered regions) of smaller sizes if any. The data show small traces of the crystalline reflexes superimposed on the overall amorphous halo of HC5 bulk sample (Fig. 1), which indicates the presence of some ordered regions presumably at nanoscale similar to reference [14]. Although the intensity of these reflections is low, their positions correspond well to the mixed  $Bi_2Se_nTe_{3-n}$  (n = 0, 0.5, 0.6, 1, 2) crystallites, identified earlier in Bi-rich Ga-Ge-Se-Te glasses.<sup>14</sup>

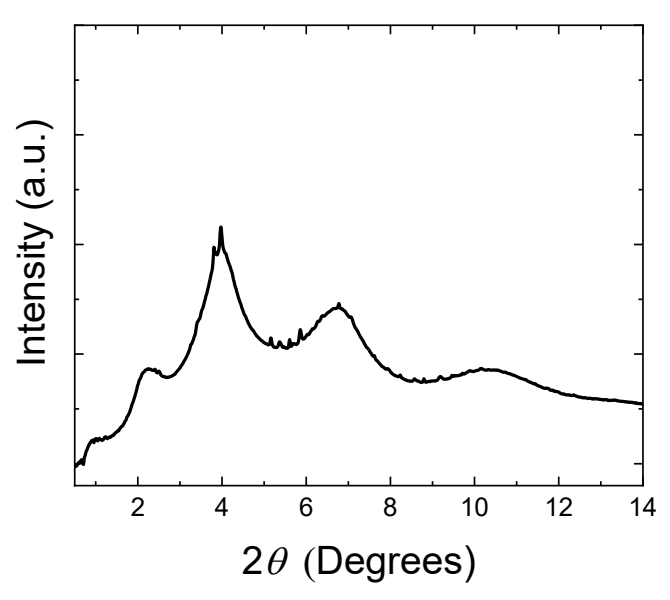


**Figure 1.** XRD pattern of HC5 bulk glass collected using synchrotron X-rays with wavelength 0.2127 Å, showing small traces of the crystalline phases superimposed on the amorphous halo.

The DSC curves recorded at different heating rates for HC0 (Fig. 2a) and HC5 (Fig. 2b) bulk glasses show glass transition at ~400-475 K and number of crystallization peaks at ~400-625 K for HC5 glass (Fig. 2b), depending on the heating rate. TOPEM® studies, which provide

true phase transformation temperatures,<sup>19</sup> show in HC5 bulk glass a non-reversible heat flow component with exotherms at ~380-410 K, 460-500 K and 520-560 K corresponding to the crystallization (Fig. 3). The non-reversible heat flow of HC0 bulk sample shows no significant endo- or exothermic peaks in the investigated temperature inteval, which agrees well with the featureless XRD patterns of HC0 bulk glass. The onset values of glass transition temperatures for HC0 and HC5 glasses determined from the reversible heat flow signal in TOPEM® measurements (Fig. 3) are both found to be close to 410 K. However, the glass transition interval for HC5 glass is wider, having endset glass transition temperature by ~35 K higher than for HC0 sample (Fig. 3). It is interesting to note, that crystallization of HC5 occurs entirely within this extended glass transition interval (Fig. 3).

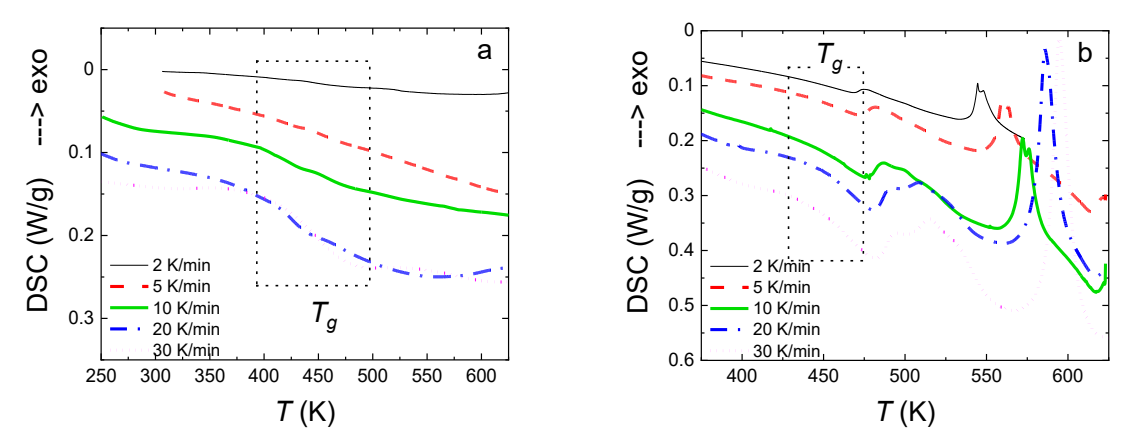


**Figure 2.** Non-isothermal conventional DSC curves recorded for HC0 (a) and HC5 (b) bulk glasses.

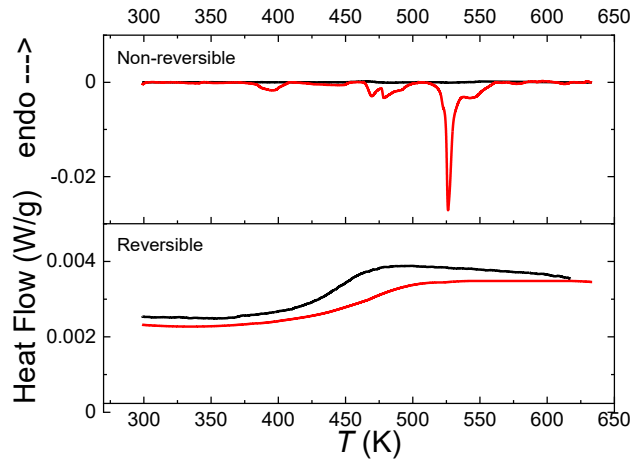


**Figure 3.** Non-reversible and reversible components of TOPEM® DSC signal recorded for HC0 (black) and HC5 (red) bulk glasses.

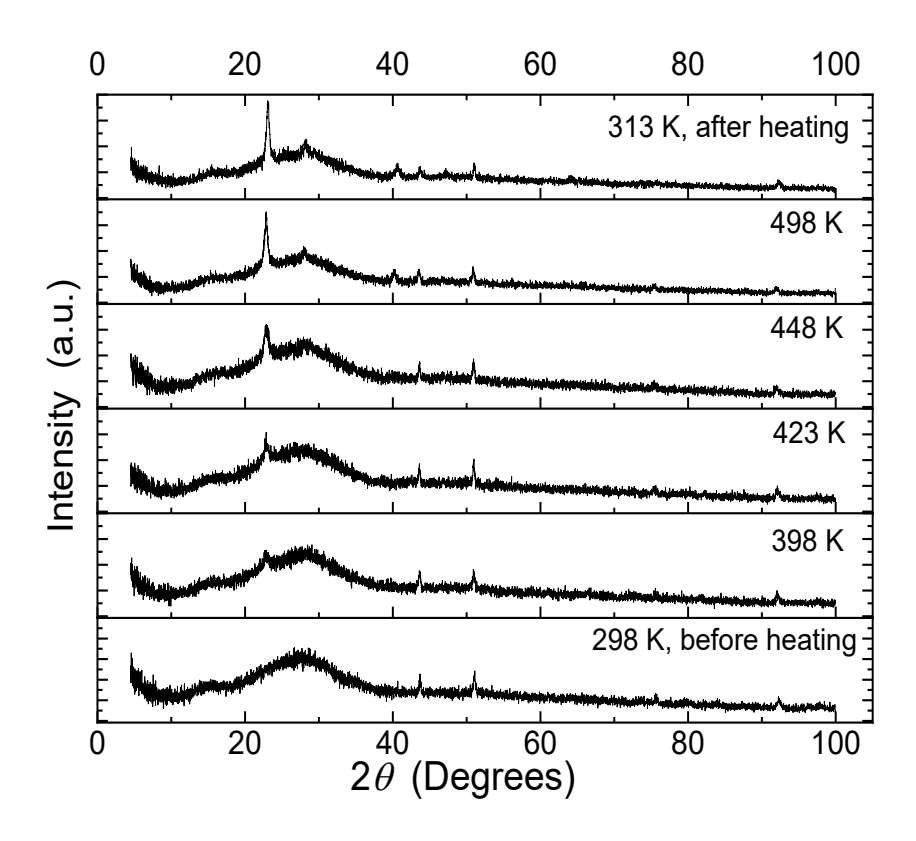


**Figure 4.** XRD patterns (Cu  $K_{\alpha}$  radiation with wavelength 1.5406 Å) collected at different temperatures for HC5 thin film deposited on microscopy slide.

Conventional (collected using Cu  $K_{\alpha}$  radiation) XRD patterns of HC0 thin films did not show any significant crystalline reflexes within the entire range of the investigated temperatures (until 453 K). Conventional XRD patterns recorded for the as-prepared HC5 thin films deposited on microscopy slides show some traces of the ordered regions already at room temperature (Fig. 4). Additional crystalline reflexes emerge in the XRD patterns of HC5 thin films when heated above ~400 K (Fg. 4). This temperature corresponds well to the exothermic peak of TOPEM® non-reversible heat component at ~380-410 K (Fig. 3), which can be associated with the beginning of crystallization of the mixed Te and Bi<sub>2</sub>Se<sub>n</sub>Te<sub>3-n</sub> (n = 0, 0.5, 1, 1.5, 2) phases. <sup>20,21</sup> At higher temperatures (~500-650 K), the GeSeTe and GeBi<sub>2</sub>Te<sub>4</sub> crystalline phases can be additionally formed. <sup>20,21</sup> The most intensive peak in the XRD pattern of HC5 film developing with temperature (Fig. 4) can be used to estimate size (*D*) of the oredered regions or crystallites associated with this particular diffraction peak, using a well-known Scherrer's relation:

$$D = \frac{0.9\lambda_{\text{Cu}}}{\beta_{\text{Cos}\theta}} \tag{3}$$

where wavelength ( $\lambda_{Cu}$ ) of Cu  $K_{\alpha}$  line is 1.54 Å,  $\theta$  is Bragg's angle, and  $\beta$  is a full width at half maximum of chosen XRD reflex.

The size of the ordered regions calculated from equation (3) and conventional XRD data in Fig. 4, increases from 0 nm at 298 K, to ~13 nm at 448 K and up to ~18 nm after 498 K heating experiment. These values indicate that nanoscale ordered regions can be purposefully created in the amorphous matrix of Bi-modified equichalcogenides by gradual annealing process in order to achieve a desired nanomodification of optical and electrical properties.

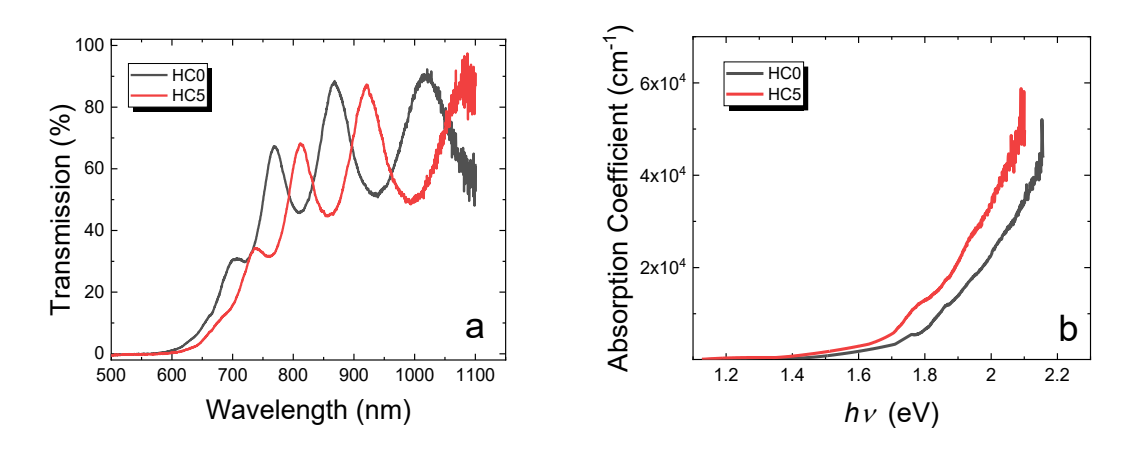


**Figure 5.** Optical transmission (a) and absorption (b) spectra (*hv* is a photon energy) recorded at room temperature for HC0 (black) and HC5 (red) thin films deposited on microscopy glass slide.

Optical transmission spectra of HC0 and HC5 thin films in the fundamental optical absorption edge region are shown in Fig. 5a. The absorption coefficient ( $\alpha$ ) calculated from the transmission data using Swanepoel theory for absorbing thin film on a transparent substrate,<sup>22</sup> follows the expected Urbach exponential behaviour (Fig. 5b) proper to the fundamental optical absorption edge of ChG. The absorption coefficient spectra were used to build Tauc plots for indirect transitions,<sup>23</sup>

$$(\alpha h \nu)^{1/2} = B^{\frac{1}{2}} (h \nu - E_g) \tag{4}$$

which provided room-temperature optical gap values  $E_g = 1.61 \ (\pm 0.01)$  eV and  $E_g = 1.58$ 

( $\pm 0.01$ ) eV for HC0 and HC5 thin films, respectively. So, incorporation of Bi leads to a decrease in optical gap of the Ge<sub>2</sub>Se<sub>3</sub>-based equichalcogenide films. This effect is similar to the behaviour of  $E_g$  in other Bi-containing Se- or Te-based binary chalcogenide compounds, like Ge<sub>30</sub>Se<sub>70-x</sub>Bi<sub>x</sub> (drops from 1.67 eV to 0.52 eV with x changing from 0 to 20),<sup>24</sup> Ge<sub>20</sub>Te<sub>80-x</sub>Bi<sub>x</sub> (drops from 0.84 eV to 0.71 eV with x changing from 0 to 7.35),<sup>25</sup> Bi<sub>x</sub>In<sub>35-x</sub>Se<sub>65</sub> (drops from 1.22 eV to 0.72 eV with x changing from 0 to 15)<sup>26</sup> or Ge<sub>20</sub>Te<sub>74-x</sub>Sb<sub>6</sub>Bi<sub>x</sub> (drops from 1.49 eV to 1.41 eV with x changing from 2 to 10).<sup>27</sup> The equichalcogenide material has a number of advantages, including the possibility to obtain it in a vitreous bulk form (which is difficult for binary systems due to a poor Bi solubility and its increased affinity to crystallization at higher concentrations), wider range for  $E_g$  variation and generally higher absolute  $E_g$  values due to simultaneous incorporation of S, Se and Te. This might be important for some applications in sensors and photonics requiring wider optical transmission window or bulk waveguides.

High relative changes in the electrical current are observed for both HC0 (Fig. 6a,b) and HC5 (Fig. 6c,d) thin films irradiated with a set of wavelengths from 400-1000 nm range. So, both matrixes are photosensitive, but incorporation of Bi decreases the photosensitivity for shorter wavelengths and lower temperature values (Fig. 6c,d). The photoexposure at the elevated temperatures increases the overall current in the films, but simultaneously decreases RCC with a cut-off at ~380 K. The RCC values go through the maximum at ~270 K for HC5 thin film (Fig. 6d), whereas a smooth decrease is observed for the HC0 thin film (Fig. 6b).

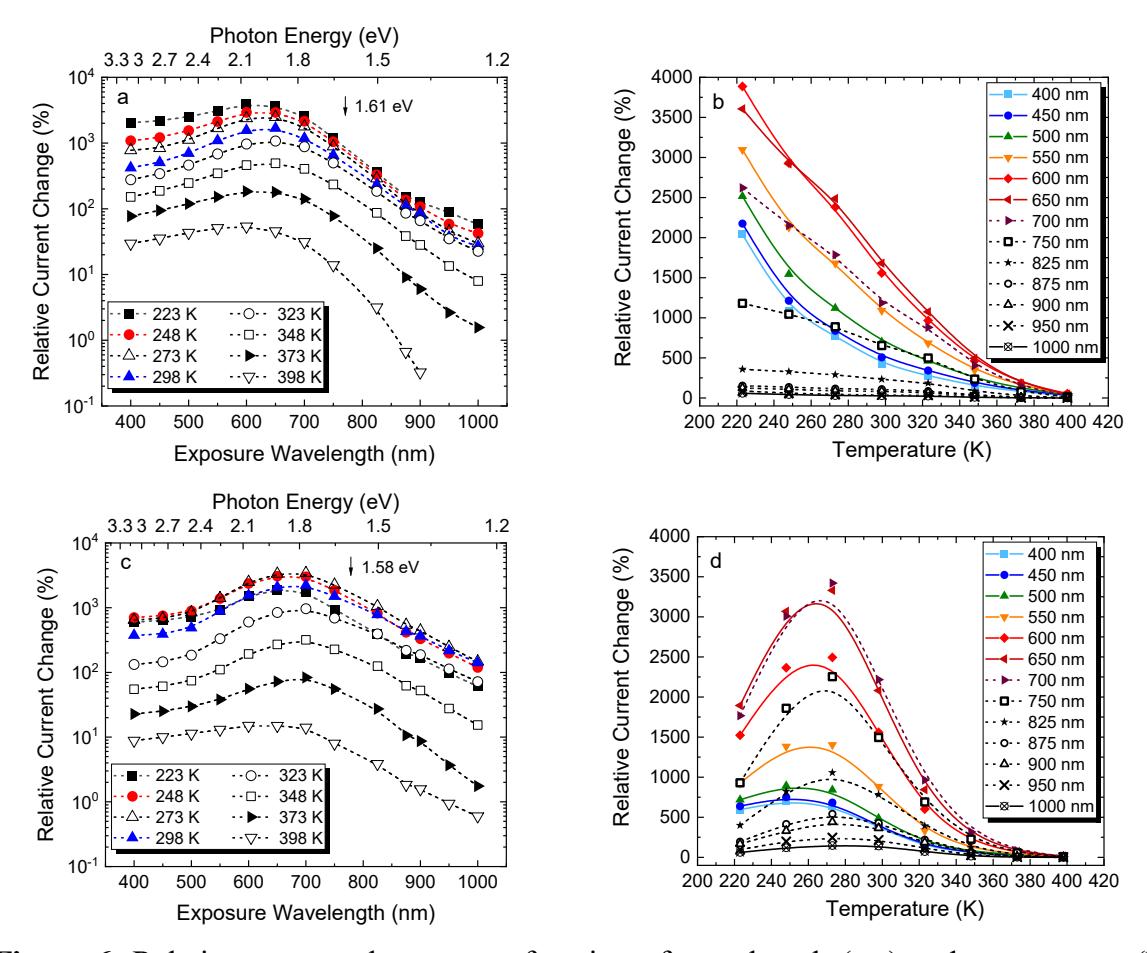


**Figure 6.** Relative current change as a function of wavelength (a,c) and temperature (b,d) measured for HC0 (a,b) and HC5 (c,d) thin films deposited on glass substrate, using 20 V bias voltage and constant flux (1.704·10<sup>16</sup> photons·s<sup>-1</sup>·cm<sup>-2</sup>) for the exposure with each wavelength. Curves are drawn as a guide to the eyes.

Temperature dependence of dark DC conductivity ( $\sigma_{DC}$ ) for bulk and thin films (Fig. 7) shows a number of differences. The overall conductivity values of thin films are ~1 order in magnitude higher than for the bulk samples, which indicates on the formation of greater number of various defects than in the bulk glass. The Bi-containing samples show higher DC conductivity at all temperatures, which correlates with the smaller optical gap and higher metallization of Bi bonds. The  $\ln(\sigma_{DC})$  vs 1/T dependence of ChG generally shows several distinct regions, which are associated with: charge carriers excited directly into non-localized states of conduction band  $E_c$  (usually high-temperature region); charge carriers excited into localized states ( $E_A$ ) near the edge of conduction band or localized states ( $E_B$ ) near the edge of the valence band ( $E_V$ ) and participating in a hopping mechanism of charge transport;

temperature-activated hopping of charge carriers localized in the states at Fermi level ( $E_F$ ); and temperature activated hopping of charge carriers with variable jump lengths (variable range hopping, which occurs usually at low temperatures and follows the well-known  $T^{-1/4}$  law).<sup>28</sup>

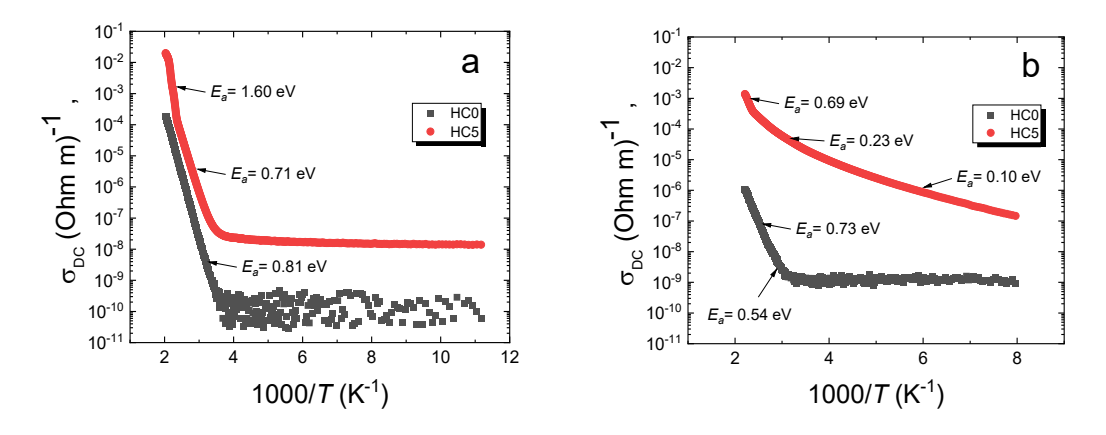


**Figure 7.** Temperature dependence of dark DC conductivity for bulk (a) and thin film (b) HC0 and HC5 samples. Activation energies are calculated from the slope of  $\ln (\sigma_{DC}) vs 1/T$  linear fits.

All these mechanisms except the low temperature one follow  $e^{-\frac{E_a}{kT}}$  dependence, where activation energy  $E_a$  depends on  $E_A$ ,  $E_B$ ,  $E_c$ ,  $E_v$ ,  $E_F$  and activation energies of charge hopping  $(W_i)$  between relevant localized states. As it follows from Fig. 7a, the  $E_a = 0.81$  eV for HC0 bulk sample corresponds to half of the optical gap, which allows us to assume (if one accepts that Fermi level in chalcogenide glasses is pinned near the middle of band gap)<sup>28</sup> that main conduction mechanism in Bi-free glass is associated with direct excitation of charge carriers into the non-localized states of conduction band with  $E_a = E_c - E_F$ . Incorporation of Bi into the bulk glass, leads to the appearance of at least two different slopes in the ln ( $\sigma_{DC}$ ) vs 1/T dependence for HC5 bulk (Fig. 7a). The major one with  $E_a = 0.71$  eV is smaller than half of the optical gap, which might indicate that Bi addition has shifted the Fermi level closer to the conduction band (again, if excitation of charge carriers into non-localized states of conduction band is considered as a main conduction mechanism), or that the hopping activation energy is involved with  $E_a = E_c - E_F + W_i$ . The second activation energy value in HC5 glass  $E_a = 1.60$ 

eV is close to the optical gap of thin films, which might indicate the conductivity mechanism originated from direct zone-zone charge carriers excitation with  $E_a = E_c - E_v$  in high-temperature regime. Temperature dependences of dark DC conductivity for thin films (Fig. 7b) show smaller activation energies and generally higher conductivity values than in bulk samples. The  $E_a = 0.73$  eV and  $E_a = 0.54$  eV for HC0 thin film are obviously smaller than half of the optical gap and must include the hopping mechanism of conduction, which indicates a higher density of localized states in this film compare to HC0 bulk glass. In Bi-modified HC5 thin film, the higher concentration of localized states is even more pronounced, owing to smaller values of the observed distinct activation energies in  $\ln (\sigma_{DC}) vs 1/T$  dependence (Fig. 7b). The observed  $\ln (\sigma_{DC}) vs 1/T$  dependence for HC5 thin film (Fig. 7b) is in good agreement with similar plots obtained for Bi-modified  $Ge_{20}Te_{80}$  ChG.<sup>25</sup> On the basis of these results, we can conclude that Bi introduces a large number of localized states into the mobility gap of equichalcogenides, which greatly enhances DC conductivity of HC5 thin film.

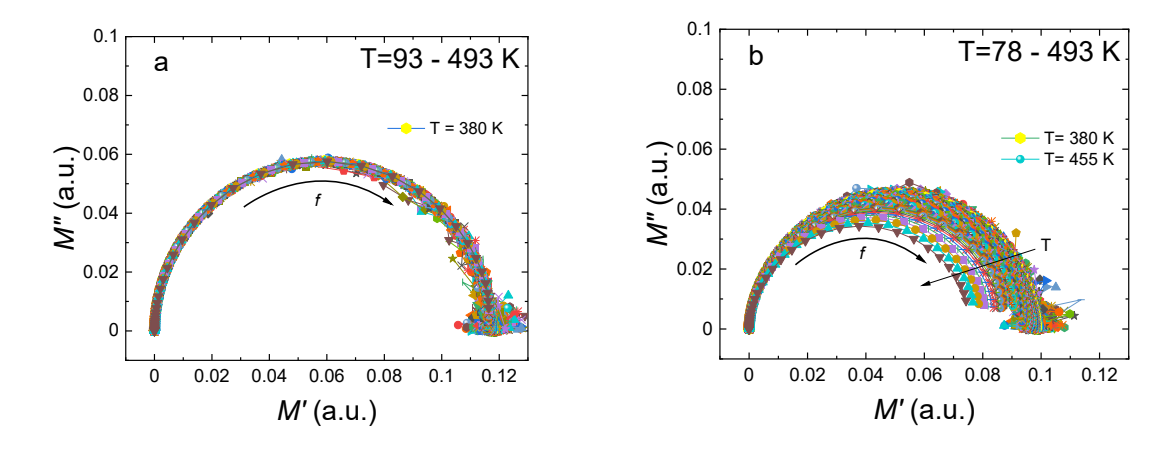


**Figure 8.** M" vs M' temperature dependences for HC0 (a) and HC5 (b) bulk samples.

The complex electric modulus spectrum derived from temperature and frequency dependences of AC conductivity can be used to identify relaxation processes in the material.<sup>29</sup> Usually, one semi-circular arc in a complex plane corresponds to a contribution from a single relaxation mechanism. The centers of the observed semi-circular arcs in Figs. 8-9 all lie on the

real axis, suggesting Debye-like type of the relaxation process in the investigated materials.<sup>29</sup> In Bi-modified bulk glass the radius of semicircle decreases after the temperature increases beyond ~380 K (Fig. 8b). On the basis of TOPEM® data in Fig. 3, this process can be associated with the appearance of ordered regions, nucleation and further crystal growth in HC5 bulk glass. It is interesting to note, that change in the radius after 380 K is not observed for the HC5 thin film (Fig. 9b) even we know the nucleation and crystallization started (Fig. 4). Instead, the Bi-containing HC5 thin film demonstrates a high-frequency and high-temperature wing developing when the temperature increases above 380 K (Fig. 9b). We believe this phenomenon is caused by a decrease with temperature in the ratio of static and optical dielectric constants as shown in reference [30]. On the basis of the obtained AC conductivity results we can speculate that crystallization in Bi-modified thin films occurs via different mechanism than in the HC5 bulk glass.

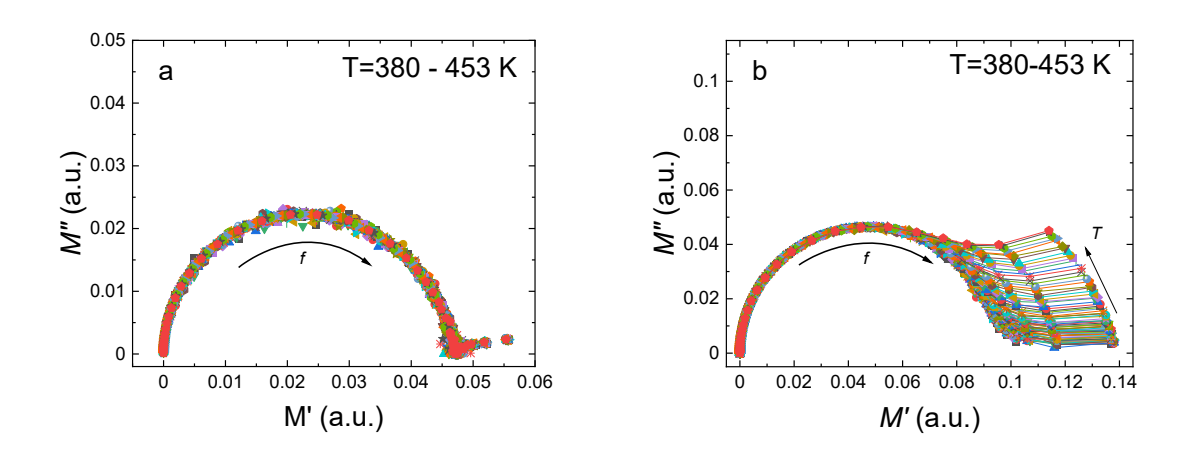


**Figure 9.** M" vs M' temperature dependences for HC0 (a) and HC5 (b) thin film samples.

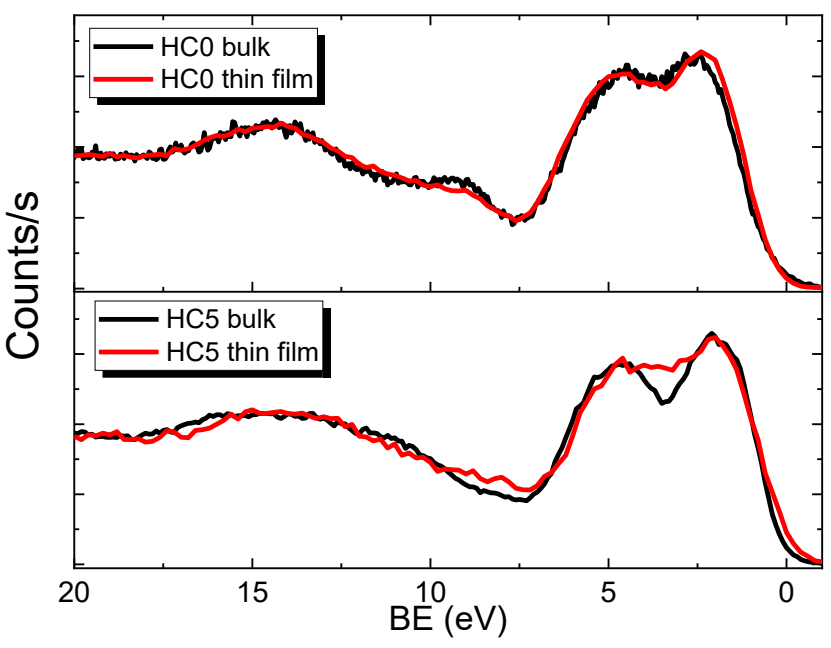
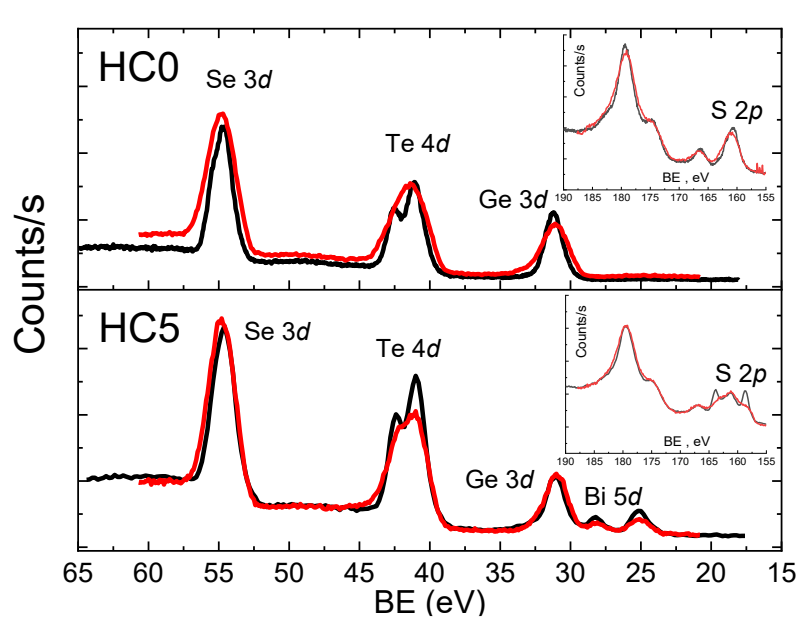


Figure 10. Valence band XPS spectra of HC0 and HC5 bulk glasses and thin films.

Important piece of the information on electronic properties of the investigated bulk and thin film materials can be obtained through the XPS valence band spectra analysis (Fig. 10). The lone pair (lp) electrons of chalcogen atoms (S, Se and Te) contribute to a density-of-state maximum at ~ 2 eV. The density-of-state maximum at about 5 eV occurs due to the broadening of S 3p, Se 4p and Te 5p bonding state peaks by the chalcogen–Ge/Bi bonds.  $^{13,31}$  Metal-metal bonds (like Ge-Ge, Ge-Bi or Bi-Bi) should have their dominant contribution at ~3.5 eV which can be ascertained from a comparison to the XPS valence band spectrum of other ChG.  $^{13,31}$  A remarkable feature of the engineered Bi-modified thin film is a higher density of states at the top of the valence band and near 3.5 eV compared to Bi-containing parent bulk glass (Fig. 10). It can explain the observed peculiarities in DC conductivity and enhanced temperature dependence of photocurrent. Availability of localized states in the band gap of the obtained thin films together with strong electron-phonon coupling proper to chalcogenide materials, are the reasons for an extended photosensitivity of these samples to the above- and below-bandgap

light (Fig. 6), which can be used in sensor applications. Obviously, the number of such states increases as we go from bulk to thin film objects, and with Bi incorporation.



**Figure 11.** Core level XPS spectra of HC0 and HC5 bulk glasses (black curves) and thin films (red curves).

Deeper XPS core-level spectra for Se 3d, Te 4d, Ge 3d, Bi 5d and S 2p electrons can be used to assess the composition and structural features of the films compare to bulk glasses. From such a comparison, it is clear that compositions of the obtained thin films are very close to the composition of the parent glasses HC0 and HC5 (Fig. 11). All core level peaks are somewhat broadened in thin films (Fig. 11), indicting an increase in structural disorder compare to bulk glasses. Exact quantification of structural fragment like it was done earlier in binary and ternary chalcogenide materials,  $^{32}$  is complicated in this case due to the increased number of possible structural entities in 4-5 component glass, as well as lack of proper reference samples at the edges of glass-forming region. In the case of S 2p core level spectra (inserts to Fig. 11), the overlap with XPS signal from Se 3p, Te 4s in HC0, and additionally with Bi 5s and Bi 4f electrons in HC5 should be considered during fitting procedure.

## **CONCLUSIONS**

Incorporation of Bi into Ge<sub>2</sub>Se<sub>3</sub>-based equichalcogenide glass matrix leads to the formation of nanoscale ordered regions in the bulk as inferred from high-energy synchrotron XRD, and an enhanced crystallization ability within glass transition region as found from DSC data. Temperature dependence of DC conductivity for bulk glasses provides one hightemperature activation energy for Bi-free glass ( $E_a = 0.81 \text{ eV}$ ) and two ( $E_a = 0.71 \text{ eV}$  and  $E_a = 0.81 \text{ eV}$ ) 1.60 eV) in the case of Bi-modified ones. Thin films prepared by vacuum thermal deposition using these bulk glasses as source materials show compositions very close to the parent bulk glasses as verified by XPS core-level spectra analysis. The films possess generally higher values of DC conductivity compare to bulk counterparts and a greater number of activation energies, indicating the abundancy of localized energy states within their mobility gap, especially in the case of Bi-containing thin films. The optical band gap is found to decrease from  $E_g = 1.61$  eV to  $E_g = 1.58$  eV in Bi-modified thin films. AC conductivity of Bi-free equichalcogenide material demonstrates one relaxation mechanism, while Bi-modified glasses and thin films possess peculiarities in complex plane dependences associated with the crystallization at higher temperatures and a change in the ratio between static and optical dielectric constants. Both HC0 and HC5 thin films are shown to be photosensitive in the visible range of spectrum, where relative changes in photocurrent reach thousands of percent depending on the exposure wavelength and temperature. Incorporation of Bi decreases the photosensitivity for shorter wavelengths and lower temperature values. Valence band XPS spectra correlate well with the observed photosensitivity, electrical and optical properties of HC0 and HC5 materials.

## **AUTHOR INFORMATION**

# **Corresponding Author**

#### Roman Golovchak\*

Department of Physics, Engineering and Astronomy, Austin Peay State University, Clarksville, TN 37044, USA

E-mail: holovchakr@apsu.edu

# **Author Contributions**

The manuscript was written through contributions of all authors. All authors have given approval to the final version of the manuscript.

# **Funding Sources**

The authors acknowledge support of National Science Foundation (NSF project OISE-2106457). TI and AT acknowledge the Joint School of Nanoscience and Nanoengineering, a member of the South-eastern Nanotechnology Infrastructure Corridor (SENIC) and the National Nanotechnology Coordinated Infrastructure (NNCI), supported by the NSF (grant ECCS-1542174).

# Notes

The authors declare no competing financial interest.

### **ACKNOWLEDGEMENTS**

APSU team acknowledges help with high-energy XRD measurements Joerg C. Neuefeind, Katharine Page, Matthew Tucker and Jue Liu.

## REFERENCES

- (1) Chalcogenide Glasses: Preparation, properties and application; Adam, J-L.; Zhang X., Eds.; Woodhead Publishing series in Electronic and Optical Materials No.44, **2014**.
- (2) Amorphous chalcogenides: advances and applications; Wang, R.P., Ed.; Pan Stanford Publishing Pte. Ltd., Singapore, **2014**.

- (3) Fritzsche, H. Why are chalcogenide glasses the materials of choice for Ovonic switching devices? *J. Phys. Chem. Solids* **2007**, *68*, 878–882.
- (4) Cui, Sh.; Chahala, R.; Shpotyuk, Ya.; Boussard, C.; Lucas, J.; Charpentier, F.; Tariel, H.; Loréal, O.; Nazabal, V.; Sire, O.; Monbet, V.; Yang, Zh.; Lucas, P.; Bureau, B. Selenide and telluride glasses for mid-infrared bio-sensing. *Proc. of SPIE* **2014**, *8938*, 893805.
- (5) Eggleton, B. J.; Luther-Davies, B.; Richardson, K. Chalcogenide photonics. *Nat. Photonics* **2011**, *5*, 141–148.
- (6) Lencer, D.; Salinga, M.; Wuttig, M. Design rules for phase-change materials in data storage applications. *Adv. Mater.* **2011**, *23*, 2030–2058.
- (7) Wang, H.; Li, W.; Wu, L.; Xue, B.; Wang, F.; Luo, Zh.; Zhang, X.; Fan, P.; Calvez, L.; Fan, B. A stable electrolyte interface with Li<sub>3</sub>PS<sub>4</sub> and Li<sub>7</sub>P<sub>3</sub>S<sub>11</sub> for high-performance solid/liquid Li-S battery. *J. Power Sources* **2023**, *578*, 233247.
- (8) Lucas, P.; Yang, Zh.; Fah, M.K.; Luo, T.; Jiang, Sh.; Boussard-Pledel, C.; Anne, M.-L.; Bureau, B. Telluride glasses for far infrared photonic applications. *Opt. Mater. Express* **2013**, *3* (8), 1049.
- (9) Feltz, A. Amorphous Inorganic Materials and Glasses; VCH, Weinheim, 1993.
- (10) Borisova, Z. U. Glassy semiconductors; Plenum Press, New York and London, 1981.
- (11) Popescu, M. *Non-crystalline chalcogenides*; Kluwer Academic Publishers, New York, **2002**.
- (12) Golovchak, R.; Plummer, J.; Kovalskiy, A.; Holovchak, Y.; Ignatova, T.; Trofe, A.; Mahlovanyi, B.; Cebulski, J.; Krzeminski, P.; Shpotyuk, Y.; Boussard-Pledel, C.; Bureau, B. Phase-Change Materials Based on Amorphous Equichalcogenides. Scientific Reports 2023, 13, 2881.
- (13) Golovchak, R.; Plummer, J.; Kovalskiy, A.; Holovchak, Y.; Ignatova, T.; Nowlin, K.; Trofe, A.; Shpotyuk, Y.; Boussard-Pledel, C.; Bureau, B. Broadband Photosensitive

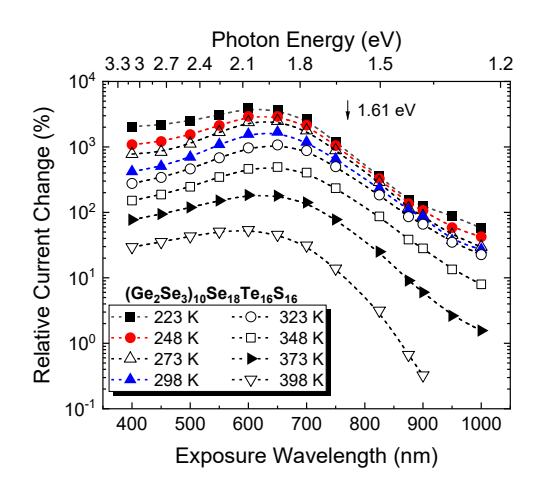
- Medium Based on Amorphous Equichalcogenides. *ACS Applied Electronic Materials* **2022**, *4*, 5397–5405.
- (14) Golovchak, R.; Shpotyuk, Ya.; Szlęzak, J.; Dziedzic, A.; Ingram, A.; Cebulski, J. Giant visible and infrared light attenuation effect in nanostructured narrow-bandgap glasses.

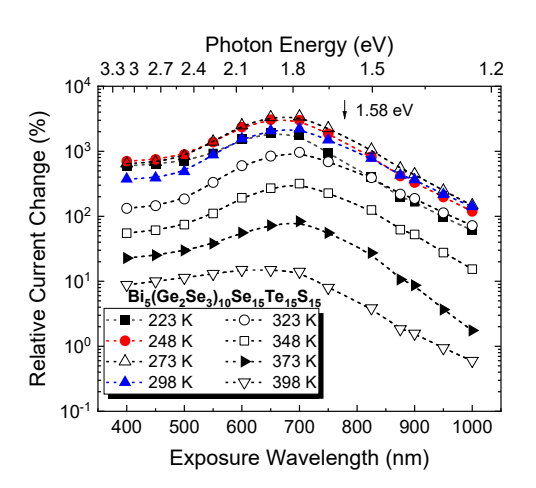
  Optics Letters 2018, 43, 387-390.
- (15) Golovchak, R.; Shpotyuk, O.; Kovalskiy, A.; Miller, A.C.; Cech, J.; Jain, H. Coordination defects in bismuth-modified arsenic selenide glasses: High-resolution x-ray photoelectron spectroscopy measurements. *Phys. Rev. B* **2008**, *77*, 172201.
- (16) Liu, Y.; Golovchak, R.; Heffner, W.; Shpotyuk, O.; Chen, G.; Jain, H. Influence of Bi on topological self-organization in arsenic and germanium selenide networks. *J. Materials Chemistry C* **2013**, *1*, 6677-6683.
- (17) Moulder, J.F.; Stickle, W.F.; Sobol, P.E.; Bomben, K.D. *Handbook of X-ray Photoelectron Spectroscopy*; Chastein, J., Ed. Perkin-Elmer Corp., Phys. Electr. Div., Eden Prairie, Minnesota, **1992**.
- (18) Conny, J.D.; Powell, C.J. Standard test data for estimating peak parameter errors in x-ray photoelectron spectroscopy III. Errors with different curve-fitting approaches. *Surf. Interface Anal.* **2000**, *29*, 856.
- (19) Schawe, J.E.K.; Hutter, T.; Heitz, C.; Alig, I.; Lellinger, D. Stochastic temperature modulation: A new technique in temperature-modulated DSC. *Thermochimica Acta* **2006**, *446*, 147–155.
- (20) Saturday, L.; Johnson, C.; Thai, A.; Szlęzak, J.; Shpotyuk, Y.; Golovchak, R. Devitrification of Bi- and Ga-containing germanium-based chalcogenide glasses. *J. Alloys Compd.* **2016**, *674*, 207–217.

- (21) Golovchak, R.; Kozdras, A.; Hodge, T.; Szlęzak, J.; Boussard-Pledel, C.; Shpotyuk, Ya.; Bureau, B. Optical and thermal properties of Sb/Bi-modified mixed Ge-Ga-Se-Te glasses. *J. Alloys and Compd.* **2018**, *750*, 721-728.
- (22) Swanepoel, R. Determination of the thickness and optical constants of amorphous silicon. *J. Phys. E: Sci. Instrum.* **1983**, *16*, 1214.
- (23) Ganjoo, A.; Golovchak, R. Computer program PARAV for calculating optical constants of thin films and bulk materials: Case study of amorphous semiconductors. *J. Optoelectronics Adv. Materials* **2008**, *10*, 1328-1332.
- (24) Aparimita, A.; Behera, M.; Sripan, C.; Ganesan, R.; Jena, S.; Naik, R. Effect of Bi addition on the optical properties of Ge<sub>30</sub>Se<sub>70-x</sub>Bi<sub>x</sub> thin films. *J. Alloys and Compounds* **2018**, 739, 997-1004.
- (25) Bhatia, K.L.; Singh, M.; Katagawas, T.; Kishoret N.; Suzukis, M. Optical and electronic properties of Bi-modified amorphous thin films of Ge<sub>20</sub>Te<sub>80-x</sub>Bi<sub>x</sub>. *Semicond. Sci. Technol.* **1995**, *10*, 65.
- (26) Priyadarshini, P.; Das, S.; Alagarasan, D.; Ganesan, R.; Varadharajaperumal, S.; Naik, R. Role of Bismuth incorporation on the structural and optical properties in Bi<sub>x</sub>In<sub>35-x</sub>Se<sub>65</sub> thin films for photonic applications. *J. Am. Ceram. Soc.* 2021, 104, 5803–5814.
- (27) Kumar, P.; Tripathi, S.K.; Sharma, I. Effect of Bi addition on the physical and optical properties of  $Ge_{20}Te_{74-x}Sb_6Bi_x$  (x = 2, 4, 6, 8, 10) thin films deposited via thermal evaporation. *J. Alloys and Compounds* **2018**, 755, 108-113.
- (28) Mott, N.F.; Davis, E.A. *Electron Processes in Non-Crystalline Materials*; Clarendon Press. Oxford, **1979**.
- (29) Ngai, K.L. Relaxation and Diffusion in Complex Systems; Springer, New-York, 2011.
- (30) Cao, W.; Gerhard, R. Calculation of various relaxation times and conductivity for a single dielectric relaxation process. Solid State Ionics **1990**, *42*, 213-221.

- (31) Kozyukhin, S.; Golovchak, R.; Kovalskiy, A.; Shpotyuk, O.; Jain, H. Valence band structure of binary chalcogenide vitreous semiconductors by high-resolution XPS. *Semiconductors* **2011**, *45*, 423-426.
- (32) Golovchak, R.; Shpotyuk, O.; Kovalskiy, A. High-resolution XPS for determining the chemical order in chalcogenide network glasses. *J. Non-Cryst. Solids X* **2023**, *18*, 100188(9).

# For Table of Contents only





Relative current change in pure and Bi-modified equichalcogenide thin films as a function of exposure wavelength at different temperatures